Annals of Mathematics and Artificial Intelligence (2024) 92:201–214
https://doi.org/10.1007/s10472-023-09885-8

A study on the predictive strength of fractal dimension of white and grey matter on MRI images in Alzheimer's disease

Niccolò Di Marco[1] · Azzurra di Palma[1] · Andrea Frosini[1] · for the Alzheimer's Disease Neuroimaging Initiative*

Accepted: 26 June 2023 / Published online: 1 August 2023

Abstract
Many recent studies have shown that Fractal Dimension (FD), a ratio for figuring out the complexity of a system given its measurements, can be used as an useful index to provide information about certain brain disease. Our research focuses on the Alzheimer's disease changes in white and grey brain matters detected through the FD indexes of their contours. Data used in this study were obtained from the Alzheimer's Disease (AD) Neuroimaging Initiative database (Normal Condition, $N=57$, and Alzheimer's Disease, $N=60$). After standard preprocessing pipeline, the white and grey matter 3D FD indexes are computed for the two groups. A statistical analysis shows that only grey matter 3D FD indexes are able to differentiate healthy and AD subjects. Although white matter 3D FD indexes do not, it is remarkable that their presence enhance the separation capability of previous ones. In order to valuate the classification capability of these indexes on healthy and AD subjects, we define several Neural Networks models. The performances of these models vary according to the statistical analysis and reach their best performances when each 3D FD input index is changed into a sequence of 2D FD indexes of (a subset of) the horizontal slices of the white and grey matter volumes.

Keywords Fractal dimension · Alzheimer's disease · Grey matter · White matter · Neural network · Brain MR imaging

Niccolò Di Marco, Azzurra di Palma and Andrea Frosini contributed equally to this work.

*Data used in preparation of this article were obtained from the Alzheimer's Disease Neuroimaging Initiative (ADNI) database (adni.loni.usc.edu). As such, the investigators within the ADNI contributed to the design and implementation of ADNI and/or provided data but did not participate in analysis or writing of this report. A complete listing of ADNI investigators can be found at: http://adni.loni.usc.edu/wp-content/uploads/how_to_apply/ADNI_Acknowledgement_List.pdf.

✉ Niccolò Di Marco
niccolo.dimarco@unifi.it

✉ Azzurra di Palma
azzurra.dipalma94@gmail.com

✉ Andrea Frosini
andrea.frosini@unifi.it

[1] Department of Matemathics and Computer Science, University of Florence, Viale Giovanni Battista Morgagni, 67/a, 50134 Florence, Italy

1 Introduction

"What we observe is not nature in itself but nature exposed to our method of questioning" wrote German physicist Werner Heisenberg, who was the first to fathom the uncertainty inherent in quantum physics. This sentence does not only apply to quantum physics but it is extendable to all scientific fields. Currently, it is now well known that Euclidean geometry can only interpret regular and smooth objects that are almost impossible to find in nature [19], so it cannot be used to quantify the white and grey matter of the brain accurately. Studying the irregular geometry of the brain is possible, as an example, thanks to fractal geometry [5]. In fact anatomical systems can be geometrically classified as natural fractals due to their irregular shape and the fact that their measures properties depend on the scale at which they are measured [38]. The results can be translated to clinical practise to help physicians in discriminating different pathologies [12], different stage of a physiopathological condition, temporal changes in the same pathology followed over time and morphological variations in anatomical structures [35]. Fractal analysis methods can be used to quantify complexity of brain activity and changes in structure of brain regions, in particular in case of Alzheimer disease [44].

Alzheimer is an irreversible neurodegenerative disease that results in a loss of mental function caused by the deterioration of brain tissue. AD is considered one of the most common causes of dementia, demonstrating progressive decline in visuo-spatial abilities, language and memory. In AD, symptoms gradually worsen over a limited number of years: in its early stages, memory loss is mild, but, with late-stage Alzheimer's, individuals lose the ability to carry on a conversation and, by degrees, respond to their environment and relatives. During the whole lifespan, cognitive abilities change increasing from childhood to midlife and then, through late middle age to old age, there is a slow and relentless decline. From a neuroanatomical point of view, AD is conceptualized primary as a progressive consequence of two hallmark pathological changes: extracellular amyloid plaques, which are composed of chains of amino acid amyloid-beta (A β), the main biological marker of AD brain, and neurofibrillary tangles, intraneuronal aggregates composed of phosphorylated τ protein [34], normally located along the axon, where it physiologically facilitates the axonal transport. Because of the distribution of this pathology and its associated neurodegeneration, AD is typically considered a disease of the brain's grey matter but, in addition to the neuronal loss characteristic of the disease, white matter degeneration and demyelination may be important pathophysiological features. Myelin loss and the inability of the oligodendrocytes [15], the cells responsible for the production and maintenance of myelin, to repair myelin damage may be additional central features of AD [6].

The relevant changes in the white and grey matter structure and extension in AD subjects may be revealed by standard measurements of the topological properties of their contours. In particular, their local and global smoothness can be investigated through *fractal dimension*, a measure that expresses how far a jagged contour locates with respect to a fractal one. Indeed, fractal dimension has been widely used to investigate the status and the evolution of the shapes of natural structures, tissues and lesions along the whole subjects' lifespan [1, 14, 33]. It was also used in case of multiple sclerosis [16], schizophrenia and manic-depressive patients [9].

Concerning the study of AD using fractal dimension, previous investigations show that subjects with AD have decreased fractal dimension (FD) in different physical structures of the brain [22, 24, 31]. These studies mainly focus on the grey matter FD, since no significant statistical correlation between white matter FD changes and AD are reported. However, since

AD degeneration involves white and grey matter, both their contours could be considered as constituted of parts that are in some ways self-similar (so presenting a fractal structure) and whose extensions are not complementary. Therefore, they can be thought as different aspects of the same degenerative process. Indeed, the present study moves from this assumption and proposes the use of three layers Neural Networks (NN) in order to improve the clusterization and classification of AD patience using both white and grey matter FD indexes. Up to our knowledge, no combined white and grey matter FD analysis is present in literature to detect brain changes related to the AD diagnosis, so the novelty of our approach both in terms of the used dataset and of the inspection and prediction methodology through a series of NN models. As a matter of fact, NNs are often used to do predictions and diagnosis in a wide range of fields, from social science to engineering and health care (for an overview on NNs models and applications see [2, 3, 37]). In principle, the NNs perform as well as conventional statistical methods, but it is not rare that they outperform in accuracy on validation samples. These advantages are related to their possibilities, as nonlinear multiple regression models, both to fit almost any nonlinear phenomenon, and to identify patterns in subsets of the input variables. The internal parameters estimation is a crucial phase in the design of a NN, and it is carried on during a sequence of training sessions where it is usually required to minimize the sum of squared errors by means of nonlinear search procedures i.e., back propagation [41], and quick propagation [17] instead of the standard least squares computation.

The aim of the present study is to investigate whether the Fractal Dimension is sensitive to change in white and grey matter of healthy and Alzheimer's brain. In particular, the FD indexes are computed after a preprocessing stage where white and grey matter of each subject are segmented. The obtained sequences are first statistically compared, both singularly and then coupled, to provide evidence of the morphological brain changes that appear during Alzheimer's disease. Then, the predictive capabilities of FD's measures are tested using a series of NN whose inputs vary from the single three dimensional FD values of the white and grey matter for each subject, to sequences of two dimensional FD values obtained by a subset of the slices of each considered MRI.

2 Materials and methods

2.1 Subjects

Data used in the preparation of this article were obtained from the Alzheimer's Disease Neuroimaging Initiative (ADNI) database (adni.loni.usc.edu). The ADNI was launched in 2003 as a public-private partnership, led by Principal Investigator Michael W. Weiner, MD. The primary goal of ADNI has been totest whether serial magnetic resonance imaging (MRI), positron emission tomography (PET), other biological markers, and clinical and neuropsychological assessment can be combined to measure the progression of mild cognitive impairment (MCI) and early Alzheimer's disease (AD). Partecipants are recruided from 63 sites in the United States and Canada, in order to collect a variety of clinical and imaging assessment.

Subjects are followed and re-examined through time to track the pathology of the disease as it progresses. ADNI was launched in 2003 as a public-private partnership, led by Principal Investigator Michael W. Weiner, MD. For up-to-date information on ADNI, visit www.adni-info.org. Results are then shared by ADNI through the *USC Laboratory of Neuro Imaging's*

Image and Data Archive (IDA) [23]. Our research included 57 healthy subjects who fulfilled the ADNI criteria for normal cognition (NC) and 60 patients with AD.

Details on the inclusion/exclusion criteria of the subjects can also be retrieved in the ADNI info website (www.adni-info.org). Here, we specify the clinical scales for the AD diagnosis: abnormal memory function score on Wechsler Memory Scale [30] (adjusted for education), Mini-Mental State Exam score between 20 and 26 [26], Clinical Dementia Rating equals 0.5 and Memory Box score at least 1.0 [29]. In addition, all the subjects are required to have a Modified Hachinski score less than or equal to 4 [28] and a geriatric Depression Scale less than 6 [43].

All the subjects were between 55 to 90 years. The ages are not statistically different between groups.

2.2 MRI acquisition

As reported in ADNI website, the MRI protocol for ADNI1 images focused on consistent longitudinal structural imaging on 1.5 T scanners using $T1$ and dual echo $T2$-weighted sequences. After the acquisition, all the images undergo quality control at Mayo Clinic in which two series of quality controls are performed, adherence to the protocol parameters and series-specific quality (i.e., subject motion, anatomic coverage, etc.). In particular, Mayo provided intensity normalized and gradient un-warped TI image volumes. The image corrections provided by ADNI are described at https://adni.loni.usc.edu/methods/mri-tool/mri-analysis/.

2.3 Preprocessing, segmentation and border extraction

We decided to perform a second series of standard preprocessing steps using the Matlab toolbox CONN [36, 45] in order to guarantee the perfect alignment and centering of the subjects in the chosen standardized space. The images also undergo a smoothing process to improve the signal-to-noise ratio and attenuate anatomical variances caused by inaccurate inter-subject registration. Then, we segmented white and grey matter in two steps, as shown in Fig. 1:

- separates brain regions from extracerebral parts;
- generates two separate images containing white matter and grey matter basically relying on the intensity values of the pixel intensities.

The segmentation of both the white and grey matter relies on [4] and it is provided by the CONN toolbox. This algorithm is considered as a standard one for general purpose studies i.e. when no lesions are present andor no specific pulse sequences are considered. The choice is motivated by the fact that, although different segmentation algorithms are present in literature, we expect that, while varying the total number of white and grey detected pixels, their distributions and mutual ratio both for the same subjects and between subjects, is not affected and similarly holds for the fractal dimensions. We stress again that the white and grey matter volumes obtained after the segmentation are not self complementary, as shown in Fig. 2.

Fig. 1 From left to right: example of an axial slice view of the original MRI not defaced in which eyes, nose and ears are perfectly visible; an axial slice view of white matter (center image) and grey matter (right image) extracted from MRI after preprocessing steps provided by Conn toolbox

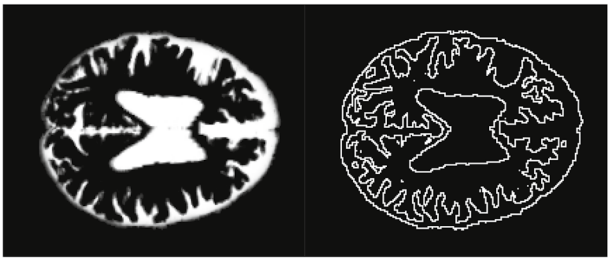

Fig. 2 On the left an axial 2D slice image of the white matter region of a MRI processed image. On the right the segmented border extraction of the same region

Finally, we extract the borders of the detected regions for the successive computation of their fractal dimensions. The extraction is performed by the Matlab function *getborder* [42] that returns the outline logical values of a binary picture using 8-connected neighborhood (see Fig. 2).

2.4 Fractal measures

Fractal dimension is a measure that indicates the complexity of an object comparing how detail in their patterns change with the scale at which it is measured.

From an algorithmic point of view, FD is measured using box-counting methods [20, 25, 39]. Box-counting methods have many good properties like robustness [24] and ability to evaluate the fractal of an object with and without self-similarity [16]. Moreover, it is possible to estimate the global complexity of a set of irregularly shaped objects, like white and grey matter.

From a mathematical point of view, box counting methods compute FD as

$$FD = \lim_{\varepsilon \to 0} \frac{log(N(\varepsilon))}{log\left(\frac{1}{\varepsilon}\right)}$$

where ε is the side of the box and $N(\varepsilon)$ is the smallest number of contiguous and non-overlapping boxes of side ε required to cover the border of the volume. Strictly speaking, box

Table 1 Summary of FD values

	White	Grey
NC	2.246 ± 0.25	2.213 ± 0.070
AD	2.240 ± 0.030	2.262 ± 0.054

Note that we compared NC and AD group both for white and grey matter. In order to apply $t-$ test, we checked that data were normally distributed and that variances of each group for each (separate) type of matter are equal. For the former we used Shapiro test while for the latter we used $F-$ test. Note that we suppose results significant when $p < 0.05$. Result are shown in Tables 2 and 3

Table 2 Shapiro test

	White	Grey
NC	0.657	0.687
AD	**0.001**	0.841

The boldface entry indicates the only significant value corresponding to $p < 0.05$

Table 3 $F-$ test

Type	White	Grey
p	0.289	0.078

Table 4 Henze-Zirkler test

Group	ND	AD
p	0.778	0.137

counting methods compute the limit by covering the object with box of decreasing length side ε. We estimate FD using *boxcount package* [18] in Matlab.

2.5 Statistical analysis

Statistical analysis were performed using packages *stats, MVN, heplots, Hotelling* in R [13, 27, 32, 40]. We investigated the measure of fractal dimension of white and grey matter in 57 healthy subjects (ND) and 60 with Alzheimer's disease (AD). Table 1 contains a summary of the values of FD for each group expressed by $mean \pm s.d.$.

The results show that $t-$ test assumptions are not satisfied for white matter in AD group. Therefore, we decided to use Wilcox test instead of $t-$ test for that case.

Then, we consider the impact of both white and grey matter FDs. In this case, each subject has associated two measurements, one for the white matter and one for the grey matter. Therefore, to evaluate differences between groups, we used a Hotelling's T-test. Also in this case, we check that assumptions hold. Specifically, data must come from a multivariate normal distribution and the covariance between the two groups must be equal. For the former we use a Henze-Zirkler (HZ) test [21] and for the latter we use a Box M-test [8]. The result of HZ are swhon in Table 4.

By the obtained results, we cannot reject the hypothesis that data comes from multivariate normal distribution. Moreover, the Box M-test gives a $p-$ value of 0.188 and therefore we do not reject the hypothesis that the two covariance matrices are equal. After these tests, we assumed that both the assumptions are satisfied.

2.6 Neural network model

The NN model selected for this study is a widely used three-layers fully-connected network whose general topology is shown in Fig. 3. The three layers have a different number of nodes, linked with weighted directed connections. In particular, the cardinality of the input layer varies according to the six input data set used in the study: 3D-White, 3D-Grey, 3D-WhiteGrey, 2D-White, 2D-Grey and 2D-WhiteGrey. The inputs 3D-White, 3D-Grey, and 3D-WhiteGrey are the three dimensional FD indexes of the white matter, the grey matter and the couple of these two indexes of all the subjects, respectively. The NNs whose inputs are the first two data sets have one single input neuron, while the latter has two input neurons. On the other hand, the inputs 2D-White, 2D-Grey and 2D-WhiteGrey are the two dimensional FD indexes of sequences of (horizontal) brain slices of the white matter, grey matter and both of them of each subject, respectively.

The slices of each MRI image are 181 and their vertical arrangement produces the whole brain volume. In order to prevent border phenomena that could lead to erroneous or non possible FD computations, we restrict the input 2D sequences (of FD indexes) to the 60 central slices only, i.e., a sufficiently large part of the 181 2D slices such that all the FD indexes are defined and enough to provide the general behaviour of the FD spatial distribution. So, the NNs whose inputs are 2D-White, 2D-Grey have 60 input neurons each, while the input neurons double to 120 in the NN that acts on 2D-WhiteGrey data.

The hidden layer's nodes may slightly vary in number according to the function to approximate: however, it is commonly accepted that their number may vary between the numbers of the input and the output neurons, with a minimum number of ten (we follow a practical rule of thumb suggested by [7]). The layers are connected by non linear *sigmoid* functions whose general form is $f(x) = \frac{1}{1+e^{-x}}$. The output layer performs the chosen categorization with one single neuron, in accordance with the binary values (0 = AD subject, 1 = healthy subject) as required.

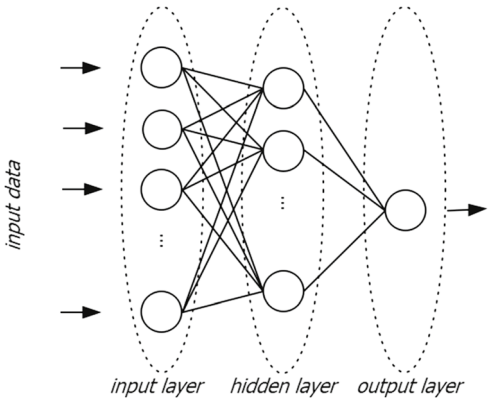

Fig. 3 Topology of the Neural Network (NN) model used in this study

Both the networks' definitions and the output are handled with the NN toolbox of Matlab. The learning algorithm seeks to minimize the error function generated on the training data to reach an acceptable level of performances, but it is not guaranteed to find a global minimum.

$$F = \frac{1}{N}\sum_{i=1}^{N}(t_i - t_{i'})^2.$$

The training of the network is performed on the 70% of the dataset, while the remaining part is equally split between the validation and test sets, following the standards.

The NN toolbox of Matlab also manages the parameters for the stop criteria, in particular the number of epochs is personalized (set to 500) while we keep the minimum performance gradient to the default value. In our study, we adopt two training strategies among the most popular and that acts quite differently, i.e., the Levenberg–Marquardt Backpropagation and the Bayesian interpolation. For each NN model, we show the average performances over about 1 K trainings on randomized training data set. We recall that the first training strategy performs a fast convergence avoiding most of the overfitting problems, while the latter tries to minimize estimation errors without penalizing the generalization capability [10].

3 Results

The white and grey matter segmented images undergo a first statistical analysis in order to detect significant correlations between their 3D fractal dimensions and the presence of AD disease. As witnessed in the literature, only the grey matter FD correlates with the AD diagnosis, while no combined white and grey matter FD analysis is present. On the other hand, different effects have been investigated between the fractal dimension of AD subjects and the changes both in the physical structures of (parts of) the brain such as gyrification index and cortical thickness [22, 24], and in the cognitive assessment obtained by standard scale-cognitive tests. After the statistical analysis, we deepen our study by investigating the predictive capabilities of our neural network models both using the single 3D FD indexes of healthy and AD subjects' white and grey matter and the sequences of their splittings into sequences of 2D FD indexes.

3.1 Statistical analysis results

A first box plot of white and grey matter FD values for healthy and AD subjects is shown in Fig. 4.

A first visual inspection reveals that grey matter of AD subjects shows higher values than healthy subjects, while no difference seems to occur in case of white matter. Statistical tests confirm these observations. Specifically, Table 5 shows the result for $t-$ test for the grey matter and Wilcox test for white matter. Concerning the first, we test the alternative hypothesis that the true difference in means between AD and healthy subjects' FDs mean values is greater than zero. Instead for Wilcox test we consider the alternative hypothesis that true location shift does not equal 0.

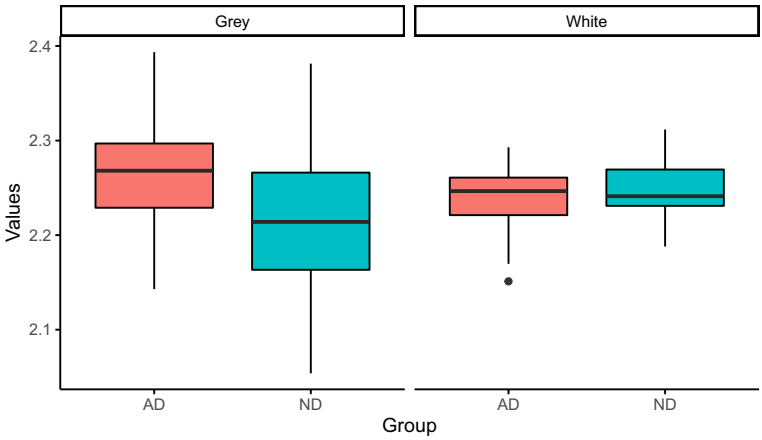

Fig. 4 Box plot of fractal dimension values of AD and healthy (ND) subjects for grey and white matter

Table 5 $p-$ values computed for Wilcox test (white matter) and $t-$ test (grey matter)

Type	White	Grey
p	0.47	< 0.001

As already observed, a significant difference is highlighted only in grey matter case. Finally, we study the behaviour offered by FD computed both on grey and white matter. In this case, each subject has associated two measurement. The Hotelling's T-test return $p < 0.001$, that lead us to accept the alternative hypothesis that the true difference in multivariate mean distributions is significantly different from zero.

3.2 Neural network models performances

The statistical analysis of the FD indexes allows us to define a series of Neural Network predictive models that are tuned according both on different series of input data and on different training algorithms, in particular we used two among the most popular, i.e. the Levenberg–Marquardt backpropagation (LM), and the Bayesian interpolation (BR). The desired output for AD subjects prediction is binary (0 = healthy subject, 1 = AD subject) according to the diagnosis provided in the ADNI database. Since the healthy and AD subjects populations are comparable in cardinality, we displayed the average performances of each network (on a 1 K trials) in terms of total recognition capability. No further normalization of the data is required.

The NN performances are presented in Fig. 5. We underline the differences between the NN8 and NN10 and the remaining NNs: the first two show good predictive performances with a very low percentage of false positive and false negative, respectively. On the other hand, the remaining NNs, but NN12, have a percentage of false positive and false negative that distribute uniformly, so accordingly to the similar cardinalities of the AD and healthy subjects.

Model NN	Training Algorithm	Input data	Recognizing performances	
NN1	LM - Backpropagation	3D-White	Total:	63%
NN2	BR - Backpropagation	3D-White	Total:	61%
NN3	LM - Backpropagation	3D-Grey	Total:	65%
NN4	BR - Backpropagation	3D-Grey	Total:	66%
NN5	LM - Backpropagation	3D-WhiteGrey	Total:	70%
NN6	BR - Backpropagation	3D-WhiteGrey	Total:	66%
NN7	LM - Backpropagation	2D-White	Total:	78%
NN8	BR - Backpropagation	2D-White	Total:	70%*
NN9	LM - Backpropagation	2D-Grey	Total:	80%
NN10	BR - Backpropagation	2D-Grey	Total:	75%*
NN11	LM - Backpropagation	2D-WhiteGrey	Total:	87%
NN12	BR - Backpropagation	2D-WhiteGrey	Total:	**

LM the Levenberg–Marquardt backpropagation, BR Bayesian regularization

Fig. 5 NN predictive performances on healthy and AD subjects. Input data are: 3D-White, i.e., FD indexes of subjects' white matter; 3D-Grey, i.e., FD indexes of subjects' grey matter; 3D-WhiteGrey, i.e., FD indexes of subjects' white and grey matter; 2D-White, i.e., sequences of sixty 2D slices FD indexes of subjects' white matter; 2D-Grey, i.e., sequences of sixty 2D slices FD indexes of subjects' grey matter; 2D-WhiteGrey, i.e., sequences of sixty 2D slices FD indexes of subjects' white and grey matter. ⋆the training process may stop with a very low false positive (NN8) or false negative (NN10) performances. ⋆⋆the Bayesian training process may fail in converging

It is worthwhile pointing out that, for each of the NN settings, the obtained predictive performances vary in accordance to the obtained statistical results. So, the NN models quantify the informative content of the data in terms of recognizability of the data set.

4 Discussions

In this study, we showed that fractal dimension computed on preprocessed MRI scans provides a valuable index to distinguish between healthy and Alzheimer's affected subjects. Because of the strong neurodegeneration that AD causes, it is commonly considered a disease of the brain's grey matter but, in addition to the neuronal loss characteristic of the disease, white matter degeneration and demyelination may be important pathophysiological

features. This is mostly related to the ability of discriminate between healthy and AD subjects shown in our study.

We stress that different algorithms have been developed to estimate the fractal dimension of natural non regular objects, also indicated as natural fractals. Here, we used the box-counting method that is commonly considered when dealing with 2D or 3D brain volumes. We first perform a statistical analysis that gives evidence of the relation between grey matter's 3D FD index and the presence of Alzheimer's disease. On the contrary, white matter's 3D FD indexes turn out to be not statistically significant related to the physical changes induced by this pathology. Finally, different to previous works, we proceed in analyzing the changes between the two previous measures and that obtained by considering both indexes at the same time. The results, obtained with a preliminary statistical analysis, corroborate the well-known observation that relevant changes occur in the borders of the grey matter regions.

To deepen the analysis, we defined a series of Neural Network models to classify healthy and AD subjects from the values of their white and grey fractal dimension indexes and compare their performances are shown in Fig. 5.

At a first sight, the inspection of the relation between the FD indexes and Alzheimer's disease showed that the performances of the NN models increase when passing from white to grey matter, in accordance with the statistical results. It is however relevant that the recognizing ability increases when the NN receives as input both the values of the FD indexes, although the statistical analysis has not been able to identify a significant relation between the white matter FD index and the AD subjects. Such a behaviour could underpin the presence of a more complex (non linear) relationship between the white matter FD index and Alzheimer's disease that has not been detected by the performed standard statistical analysis.

More specifically, we consider the first six NNs, i.e., from NN1 to NN6 in Fig. 5, that act on the aggregate 3D FD data computed on the whole brain volume of each subject MRI. We found that the predictive performances slightly increase when shifting from the 3D FD indexes of the white matter to those of the grey matter, until reaching the maximum when both indexes are considered. We notice that the choice of the training algorithm does not significantly affect the performances of the NN models. Although the recognizing performances turn out to be quite low on these data sets, it is remarkable that the percentages of false positives and false negatives detected after the six training processes locate very close (one or two points at most) to the general performances.

Finally, consider the last six NN models, i.e., from NN7 to NN12 in Fig. 5, that act on the sequences of 2D FD data computed on a subset of the horizontal slices of each MRI brain scan. We immediately realize that the performances of the NN models increase when considering the spatial vertical variation of the 2D FD indexes both in the case of white and grey matter. This observation is in accordance with the literature: as a matter of fact the AD disease performs heavy atrophic modifications, even in its first stage, on the borders of specific regions of the brain that locate in its central part, such as hippocampal region, cingulate gyri, and medial temporal lobe [11] and that can be revealed when focusing on them.

A further remark concerns the length of the input data sequences that seems to prevent the Bayesian training algorithm from performing at his best. In particular, we note that the training process may end with a huge number of false positives or false negatives, making clear that, in some cases, the presentation of the input data drives the Bayesian regularization to step into a local minimum where almost all the sequences are assigned to the same class.

This remark is also supported by the excellent performances of NN9 and NN11 trained using the Levenberg-Marquard backpropagation on the same data sets, and whose

misclassified subjects distribute uniformly, so accordingly to the similar cardinalities of the AD and healthy subjects.

Finally, a last observation concerns the longest input data 2D-WhiteGrey: the model NN11 reaches the best performances here, enhancing the mutual benefit of the white and grey matter 2D FD indexes on the separation process. On the other hand, the Bayesian regularization process fails in converging in almost all the trials. As a matter of fact, convergence rate of training algorithms for neural networks is heavily affected by the initialization of weights, so it could be worth exploiting different starting weights settings, that may vary from the simple random weight initialization to Kalman filters or Bayesian estimation, to lead the BR training to the final convergence.

Acknowledgements Data collection and sharing for this project was funded by the Alzheimer's Disease Neuroimaging Initiative (ADNI) (National Institutes of Health Grant U01 AG024904) and DOD ADNI (Department of Defense award number W81XWH-12-2-0012). ADNI is funded by the National Institute on Aging, the National Institute of Biomedical Imaging and Bioengineering, and through generous contributions from the following: AbbVie, Alzheimer's Association; Alzheimer's Drug Discovery Foundation; Araclon Biotech; BioClinica, Inc.; Biogen; Bristol-Myers Squibb Company; CereSpir, Inc.; Cogstate; Eisai Inc.; Elan Pharmaceuticals, Inc.; Eli Lilly and Company; EuroImmun; F. Hoffmann-La Roche Ltd and its affiliated company Genentech, Inc.; Fujirebio; GE Healthcare; IXICO Ltd.; Janssen Alzheimer Immunotherapy Research & Development, LLC.; Johnson & Johnson Pharmaceutical Research & Development LLC.; Lumosity; Lundbeck; Merck & Co., Inc.; Meso Scale Diagnostics, LLC.; NeuroRx Research; Neurotrack Technologies; Novartis Pharmaceuticals Corporation; Pfizer Inc.; Piramal Imaging; Servier; Takeda Pharmaceutical Company; and Transition Therapeutics. The Canadian Institutes of Health Research is providing funds to support ADNI clinical sites in Canada. Private sector contributions are facilitated by the Foundation for the National Institutes of Health (www.fnih.org). The grantee organization is the Northern California Institute for Research and Education, and the study is coordinated by the Alzheimer's Therapeutic Research Institute at the University of Southern California. ADNI data are disseminated by the Laboratory for Neuro Imaging at the University of Southern California.

Funding Open access funding provided by Università degli Studi di Firenze within the CRUI-CARE Agreement.

Data availability The data used in this study belong to the *Alzheimer's Disease Neuroimaging Initiative (ADNI)*, a neuroscience consortium of universities and research institutes, and are available through the ADNI database *(adni.loni.usc.edu)* after approval of a data request application. For more information about how to access ADNI data see http://adni.loni.usc.edu/datasamples/accessdata/.

Declarations

Conflict of interest The authors declare that they have no conflict of interest.

References

1. Abu-Eid, E., Landini, G.: Quantification of the global and local complexity of the epithelial-connective tissue interface of normal, dysplastic, and neoplastic oral mucosae using digital imaging. Pathol. Res. Pract. **199**, 475–482 (2003)

2. Ananda Rao, M., Srinivas, J.: Neural networks: Algorithms and applications. Alpha Science International (2003)
3. Arbib, M.A.: The handbook of brain theory and neural networks. MIT Press, Cambridge (2003)
4. Ashburner, J., Friston, K.J.: Unified segmentation. Neuroimage **26**(3), 839–851 (2005)
5. Baish, J.W., Jain, R.K.: Fractals and cancer. Cancer Res. **60**, 3683–3688 (2000)
6. Bartzokis, G.: Alzheimer's disease as homeostatic responses to age-related myelin breakdown. Neurobiol. Aging **32**, 1341–1371 (2011)
7. Bishop, C.M.: Neural networks for pattern recognition. Oxford University Press, Oxford (1995)
8. Box, G.E.P.: A general distribution theory for a class of likelihood criteria. Biometrika **36**(3–4), 317–346 (1949). https://doi.org/10.1093/biomet/36.3-4.317
9. Bullmore, E., Brammer, M., Harvey, I., Persaud, R., Murray, R., Ron, M.: Fractal analysis of the boundary between white matter and cerebral cortex in magnetic resonance images: a controlled study of schizophrenic and manic-depressive patients. Psychol. Med. **24**, 771–781 (1994)
10. Burden, F., Winkler, D.: Bayesian regularization of neural networks. Methods Mol. Biol. **458**, 25–44 (2008)
11. Chételat, G., Desgranges, B., De La Sayette, V., Viader, F., Eustache, F., Baron, J.C.: Mapping gray matter loss with voxel-based morphometry in mild cognitive impairment. NeuroReport **13**(15), 1939–1943 (2002). https://doi.org/10.1097/00001756-200210280-00022
12. Cross, S.S.: Fractals in pathology. J. Pathol. **182**, 1–8 (1988)
13. Curran, J., Hersh, T.: Hotelling: Hotelling's Test and Variants. R package version 1.0-8. https://CRAN.R-project.org/package=Hotelling (2022)
14. Di Ieva, A., Grizzi, F., Ceva-Grimaldi, G., Russo, C., Gaetani, P., Aimar, E., Levi, D., Pisano, P., Tancioni, F., Nicola, G., Tschabitscher, M., Dioguardi, N., Baena, R.R.: Fractal dimension as a quantitator of the microvasculature of normal and adenomatous pituitary tissue. J. Anat. **211**(5), 673–680 (2007)
15. Erten-Lyons, D., Woltjer, R., Kaye, J., Mattek, N., Dodge, H.H., Green, S., Tran, H., Howieson, D.B., Wild, K., Silbert, L.C.: Neuropathologic basis of white matter hyperintensity accumulation with advanced age. Neurology **81**, 977–983 (2007). https://doi.org/10.1212/WNL.0b013e3182a43e45
16. Esteban, F.J., Sepulcre, J., de Miras, J.R., Navas, J., de Mendizábal, N.V., Goñi, J., Quesada, J.M., Bejarano, B., Villoslada, P.: Fractal dimension analysis of grey matter in multiple sclerosis. J. Neurol. Sci. **282**(1), 67–71 (2009)
17. Fahlman, S.E.: An empirical study of learning speed in back-propagation networks. Project report CMU-CS- 88-162 (1989)
18. Moisy, F.: boxcount. MATLAB Central File Exchange. https://www.mathworks.com/matlabcentral/fileexchange/13063-boxcount (2022)
19. Goldberger, A.L., West, B.J.: Fractals in physiology and medicine. Yale J. Biol. Med. **60**, 421–435 (1987)
20. Hall, P., Wood, A.: On the performance of box-counting estimators of fractal dimension. Biometrika **80**(1), 246–251 (1993)
21. Henze, N., Zirkler, B.: A class of invariant consistent tests for multivariate normality. Commun. Stat. Theory Methods **19**, 3595–3617 (1990)
22. Im, K., Lee, J.M., Yoon, U., Shin, Y.W., Hong, S.B., Kim, I.J., Kwon, J.S., Kim, S.I.: Fractal dimension in human cortical surface: multiple regression analysis with cortical thickness, sulcal depth, and folding area. Hum. Brain Mapp. **27**, 994–1003 (2006)
23. Jack, C.R., Jr., Bernstein, M.A., Fox, N.C., Thompson, P., Alexander, G., Harvey, D., Borowski, B., Britson, P.J., Whitwell, J.L., Ward, C., Dale, A.M., Felmlee, J.P., Gunter, J.L., Hill, D.L., Killiany, R., Schuff, N., Fox-Bosetti, S., Lin, C., Studholme, C., DeCarli, C.S., Weiner, M.W.: The Alzheimer's Disease Neuroimaging Initiative (ADNI): MRI methods. J. Magn. Reson. Imaging: JMRI **27**(4), 685–691 (2008). https://doi.org/10.1002/jmri.21049
24. Jiang, J., Zhu, W., Shi, F., Zhang, Y., Lin, J., Jiang, T.: A robust and accurate algorithm for estimating the complexity of the cortical surface. J. Neurosci. Methods **172**(1), 122–130 (2008)
25. Li, J., Du, Q., Sun, C.: An improved box-counting method for image fractal dimension estimation. Pattern Recognit. **42**(11), 2460–2469 (2009)
26. Folstein, M.F., Folstein, S.E., McHugh, P.R.: Mini-mental state. A practical method for grading the cognitive state of patients for the clinician. J. Psychiatr. Res. **12**, 189–198 (1975)
27. Fox, J., Friendly, M., Monette, G.: Visualizing tests in multivariate linear models R package version 1.3-9. https://CRAN.R-project.org/package=heplots (2021)
28. Hachinski, V.C., Iliff, L.D., Zilhka, E., et al.: Cerebral blood flow in dementia. Arch. Neurol. **32**, 632–637 (1975)
29. Hughes, C.P., Berg, L., Danziger, W.L., Coben, L.A., Martin, R.L.: A new clinical scale for the staging of dementia. Psychiatry **140**, 566–572 (1982)

30. Kaufman, A.S., Lichtenberger, E.: Assessing adolescent and adult intelligence, 3rd edn. Wiley, Hoboken (NJ) (2006)
31. King, R.D., Brown, B., Hwang, M., Jeon, T., George, A.T.: Fractal dimension analysis of the cortical ribbon in mild Alzheimer's disease. Neuroimage **53**, 471–479 (2010). https://doi.org/10.1016/j.neuroimage.2010.06.050
32. Korkmaz, S., Goksuluk, D., Zararsiz, G.: MVN: An R package for assessing multivariate normality. R J. **6**(2), 151–162 (2014)
33. Landini, G., Rippin, J.: Fractal dimension of the epithelial connective tissue interfaces in premalignant and malignant epithelial lesions of the floor of the mouth. Anal. Quant. Cytol. Histol. **15**, 144–149 (1993)
34. Lee, S., Viqar, F., Zimmerman, M.E., Narkhede, A., Tosto, G., Benzinger, T.L., Marcus, D.S., Fagan, A.M., Goate, A., Fox, N.C., Cairns, N.J., Holtzman, D.M., Buckles, V., Ghetti, B., McDade, E., Martins, R.N., Saykin, A.J., Masters, C.L., Ringman, J.M., Ryan, N.S.: Dominantly inherited Alzheimer network: White matter hyperintensities are a core feature of Alzheimer's disease: evidence from the dominantly inherited Alzheimer network. Ann. Neurol. **79**(6), 929–939 (2016). https://doi.org/10.1002/ana.24647
35. Mandelbrot, B.B.: The fractal geometry of nature. Freeman, New York (1982)
36. Nieto-Castanon, A.: Handbook of functional connectivity Magnetic Resonance Imaging methods in CONN. Hilbert Press, Boston (2020)
37. Nikolaev, N.Y., Iba, H.: Adaptive learning of polynomial networks: Genetic programming, backpropagation and Bayesian methods. Springer, New York (2006)
38. Nonnemacher, T.F., Losa, G.A., Merlini, D., Weibel, E.R.: Fractals in biology and medicine, vol. I. Birhkäuser Press, Basel (1994)
39. Panigrahy, C., Seal, A., Mahato, N.K., Bhattacharjee, D.: Differential box counting methods for estimating fractal dimension of grey-scale images: A survey. Chaos Solitons Fractals **126**, 178–202 (2019)
40. R Core Team. R: A language and environment for statistical computing. R Foundation for Statistical Computing, Vienna, Austria. URL https://www.R-project.org/ (2021)
41. Rumelhart, D. E., McClelland, J., The PDP Research Group (Eds.): Parallel distributed processing. Cambridge: The MIT press (1986)
42. Schwanghart, W.: getborder. MATLAB Central File Exchange. https://www.mathworks.com/matlabcentral/fileexchange/12303-getborder (2022). Accessed 26 May 2022
43. Sheikh, J.I., Yesavage, J.A., Brooks, J.O., et al.: Proposed factor structure of the geriatric depression scale. Int. Psychogeriatr. **3**(1), 23–28 (1991)
44. Villamizar, J., Uribe, L., Cerquera, A., Prada, E., Prada, D., Alvarez, M.: Fractal analysis of neuroimaging: comparison between control patients and patients with the presence of Alzheimer's disease. J. Phys.: Conf. Ser. **2159**(1), (2022)
45. Whitfield-Gabrieli, S., Nieto-Castanon, A.: Conn: A functional connectivity toolbox for correlated and anticorrelated brain networks. Brain Connectivity **2**(3), 125–141 (2012)